Biomimetic material functionalized mixed matrix membranes for enhanced carbon dioxide capture

Yiming Zhang,[a] Huixian Wang,[b] Siyu Zhou,[a] Jing Wang,[a] Xuezhong He,[c] Jindun Liu[a]

and Yatao Zhang*[a]

[a] *School of Chemical Engineering and Energy, Zhengzhou University, Zhengzhou 450001, China*

b School of Civil Engineering and Communication, North China University of Water Resources and Electric Power, Zhengzhou 450045, China

[c] Department of Chemical Engineering, Norwegian University of Science and Technology, Norway

*Corresponding author:

Tel.: +86-371-67781734; **Fax**: +86-371-67739348

E-mail: zhangyatao@zzu.edu.cn

Abstract

Carbonic anhydrase (CA) has been widely used in gas separation membranes because of its high affinity for CO2molecules. In this work, a novel biomimetic material (Co-2,6-bis(2-benzimidazolyl)pyridine, CoBBP) which has a similar molecular structure to the CA enzyme but with higher stability and a lower price was successfully synthesized. The excellent thermal stability, dispersibility and high CO 2 selectivity make CoBBP a promising alternative to CA. Then, a series of Pebax–CoBBP mixed matrix membranes were constructed to explore their capability for CO2/N2 separation. Compared to the pristine Pebax-1657, the Pebax–CoBBP mixed matrix membrane with the optimized 1.33 wt% CoBBP loading showed an improved CO2 permeability of 675.5 barrer and a CO2/N2 selectivity of 62, surpassing the Robeson upper bound (2008). Furthermore, the hydrogen bonds between CoBBP and polyamide chains improved the chain stiffness of the linear glassy polymer, ensuring good operational mechanical stability. In short, this work could provide a promising method to exploit alternatives to the CA enzyme and to fabricate biomimetic membranes.

Keywords: biomimetic material; mixed matrix membranes; CO_2 capture; biomimetic-biological membrane reactors

Graphical Abstract

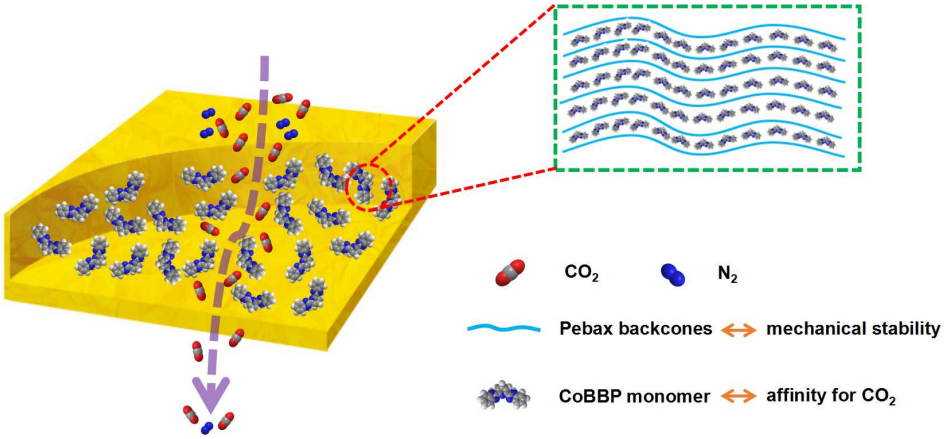

1. Introduction

Among the numerous CO_2 capture and storage (CCS) technologies, the membrane separation technology has become one of the most promising methods owing to its high CO_2 capture efficient, low energy requirement and simple operation.[1-3] At present, compared with the inorganic materials, polymers have been the commercial materials applied for gas separation on account of the scalable production and ease of manufacture. However, the polymer based membranes face the trade-off relationship between the gas permeability and selectivity (the well-known Robeson upper bond).[4, 5] In order to break through the restriction of the Trade-off effect, the explorations of new membrane materials, including the MOFs, polymers with intrinsic microporosity (PIMs), carbon molecular sieves, zeolites and other 2D materials,[6-10] are of great interests in recent years. Furthermore, a series of modifications for polymeric membrane including blending and crosslinking are used to solve the mentioned problems. Mixed matrix membranes (MMMs), incorporating the permeable or impermeable fillers into the polymeric materials, have experienced a extensively studies for gas separation in recent years.[11, 12] This kind of membranes can combine the continuous polymer phase with the nanofillers of superior gas separation efficiently, and the synergistic effect of the polymer and nanofillers can promote the gas separation. Therefore, the membrane has the potential to overcome the limitation of the Robeson upper-bound line.[13-15]

Nowadays, more and more researchers have devoted themselves to investigate the biological membranes and the combination of bio-materials and membranes. Enzymes,

refer to the catalytic function of biological macromolecules, can promote the biocatalytic process efficiently. For instance, with the help of laccase, Hou and his co-workers applied the enzymatic membrane reactor (EMR) for the efficient wastewater treatment.[16-18] Carbonic anhydrase (CA), a kind zinc enzyme with the fastest catalyze rate that can catalyze the reversible of hydration of CO_2 efficiently, has the maximal hydration factor (in excess of 10^6 s^{-1}).[19, 20] In our previous work, CA embedded ZIF-8 was used as the crystal seeds and in-situ growth on the halloysite nanotubes (HNTs) layer, and the composite membranes showed high CO_2/N_2 separation performance.[21] However, considering the ease of inactivation and the high cost, the natural CA enzymes bear some other unavoidable disadvantages, such as the sensitivity of catalytic activity under harsh environment, the poor recovery from the reaction media.[22] So, the CA is difficult to be widely extended to implement CO_2 capture at a viable industrial scale.[23]

Under these circumstances, the biomimetic materials have developed extensively in recent years. Especially the design of the biomimetic CA, it has received growing interest as a potential alternative in the CO_2 hydration field.[24-26] As shown in the structure of CA (Fig. 1a), the active site contains the Zn^{2+} that coordinated three imidazole groups and one water molecule.[27, 28] As the active site of the CA, the His_3ZnOH acts as the active substance, Zn^{2+} and the imidazole rings play the main role on the hydration of CO_2.[29] Several groups have demonstrated the activation of CO_2 in small molecules via simulating the active site of CA.[30, 31] Sahoo et al., investigated the CO_2 hydration with the help of Zn-histidine complex.[32] To date, Lee

and co-works is the only group, using MOFs packaged an organometallic compound to show a CO_2 affinity activity analogous to the active CA enzyme.[24] Over approximately the past years, metal complexes have been used to simulate the active site of CA, and showed similar activity compared to that of CA.[33-35] However, to our best knowledge, there is only one literature reported the application of biomimetic enzyme on membranes. Wang et al., used the biomimetic material-poly(N-vinylimidazole)-zinc complex on the polysulfone (PS) ultrafiltration membrane for effective CO_2 separation.[25] At present, the biomimetic enzyme on membranes has rarely been reported. Therefore, developing new biomimetic MMMs reactor paradigm is significantly required to expand the application in CO_2 capture , and the biomimetic enzyme has a bright future in the field. As well, we expect this method that can be extended to other bionic areas.

In this study, a novel biomimetic material (?) with the similar structure of CA was successfully synthesized and showed similar catalytic capability for CO_2 relative to CA. (Fig. 1b) After that, this biomimetic material was introduced into polymer matrix to make MMMs for CO2 capture. Herein, a common polymer material (Pebax-1657) was selected as the continuous phase to combine the biomimetic material effectively. On one hand, polymers based CO_2 capture are the most frequent membrane materials, which have been widely employed in conventional industry fields. Pebax-1657, a commercial rubbery copolymer with high gas permeability and selectivity, is regarded as an ideal membrane material for the capture of CO_2 from natural gas and flue gas.[36, 37] More importantly, the CoBBP can process poor compatibility in most solution in

addition to Pebax-1657. The chemical structure of Pebax-1657 is shown in Fig. 1c**.** It consists of a hard segment (PA) and a soft segment (PEO). PA segment shows the strong mechanical strength because of the high crystallinity, and the PEO as the CO_2-philic segment displays high CO_2 permeability capability due to the chain mobility and the high affinity with polar molecules.[38, 39] Therefore, this motivates our interest in choosing Pebax for the fabrication of biomimetic MMMs reactor.

In this work, the coordination of metal ion (cobalt) with 2,6-bis(2-benzimicdazoly) pyridine (named as BBP) was used to mimic the active site of CA. (Fig. 1c) This biomimetic material (CoBBP) was mixed into Pebax-1657 polymer to fabricate the MMMs via a solvent casting method. The effect of different loadings on CO_2 permeability was also investigated. The resulting membranes showed the increasing permeability of CO_2 relative to the pristine Pebax membranes. Importantly, the MMMs surpassed the Robeson upper bond in 2008. In addition, the thermal stability of MMMs modified with CoBBP was studied via a series of high temperature treatments to understand the high temperature resistance than CA. Finally, the long-term stability of the MMMs was explored to test the anti-aging behavior.

2. Experimental.

2.1. Materials

2,6-Bis(2-benzimidazolyl)pyridine (BBP) was purchased from Sigma-Aldrich. Commercial Pebax-1657 (consisting of 60 wt% polyether segments and 40 wt% polyamide segments) was obtained from Arkema Inc. Zinc perchlorate hexahydrate ($Zn(ClO_4)_2{\cdot}6H_2O$, Mw: 372.38, Purity: 99.97wt%) was purchased from Aladdin. Cobalt

perchlorate hexahydrate ($Co(ClO_4)_2 \cdot 6H_2O$, Mw: 365.93) was purchased from Shanghai Macklin Biochemical Co., Ltd. Methanol and ethanol were obtained from Medicine Group Chemical Reagent Co., Ltd and Tianjin Kermel Chemical Reagent Co., Ltd, respectively. Deionized (DI) water was used in all experiments. All the reagents have the grade of analytical standard and were used without further purification.

2.2. Synthesis of CoBBP.

2,6-Bis(2-benzimidazolyl)pyridine (BBP, 62mg) and $Co(ClO_4)_2 \cdot 6H_2O$ (73mg) were completely dissolved in methanol (10mL) via the ultrasonic treatment, separately. Then the two solutions were mixed and transferred into the round bottom flask at 60°C, the reaction time was 4h under stirring and refluxing.(Fig. 1d) The color of the mixed solution was changed from pink to orange immediately, which demonstrated the formation of the complex of the metal with the ligand. Consequently, the powder of the CoBBP was collected via the centrifugation at 10000 rpm, and then dried under vacuum at 50°C for 24h.

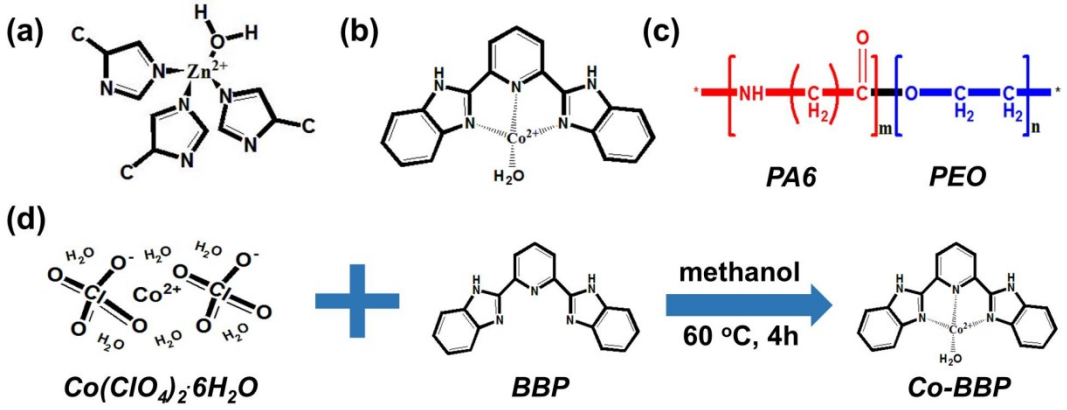

Fig. 1. Chemical structures of (a) CA; (b) CoBBP and (c) Pebax-1657; (d) the synthesis process of biomimetic material CoBBP.

2.3. Fabrication of Pebax solution and MMMs.

In this work, a certain amount of CoBBP powers were dispersed in ethanol/H_2O (70/30 of the mass ratio) solvent under the condition of sonication for 30min. Then 3g of Pebax-1657 pellets were dissolved in the above solution under reflux (80°C) for 2h. The obtained solution was standing for further use.

The biomimetic MMMs were fabricated via a solution-casting method. In short, before MMMs preparation, the casting solution was further sonicated for 30 min to remove the air bubbles at room temperature. Subsequently, a set of obtained constant-volume casting solution (to control the membrane thickness) with different contents of CoBBP were poured into PTFE petri dish The film was dried at ambient for 24h, and further kept in the vacuum oven for 24h. The preparation process is shown in Fig. 2. The obtained MMMs were denoted as Pebax-CoBBP(x), (x represented the weight percentage of CoBBP over Pebax, where x=0.33wt%, 0.67wt%, 1.0wt% and 1.33wt%) The thicknesses of all membranes were measured by a micrometer caliper for several times at different regions, which were found within 75-90 μm.

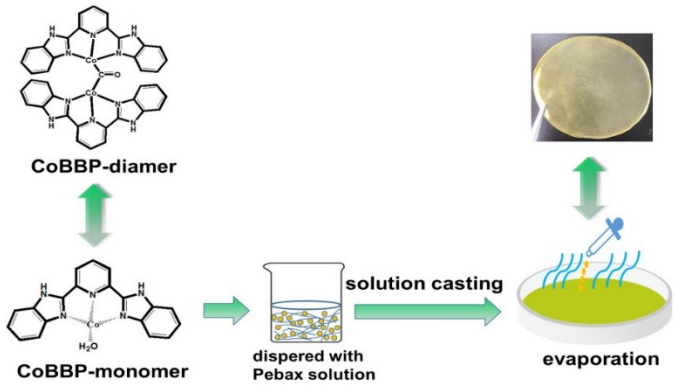

Fig. 2. Schematic diagram of the synthesis process of Pebax-CoBBP mixed matrix membranes.

2.5. Characterization of CoBBP.

The morphologies of CoBBP were characterized via transmission electron microscopy

(TEM) on a FEI model Talos F200S on a work acceleration voltage of 200 kV.

X-ray diffraction (XRD) characterization was conducted using a PAN Alytical X'pert pro (PAN alytical, The Netherlands) the scanning range of 2θ between 5° and 80° using Cu Kα as the source of radiation.

Fourier transform infrared (FTIR) analysis was carried out using MAGNA-560 manufactured by Thermo Nicolette Corporation (U.S.A.), FTIR spectrums were obtained in the range of wavenumbers from 4000 to 1500 cm^{-1} with a scan per sample.

Thermogravimetric Analysis (TGA) of CoBBP was performed using a STA 449 F3 Jupiter® (NETZSCH, Germany). Samples were heated from 25ºC to 800ºC at a heating rate of 10ºC/min under nitrogen purge gas. Moreover, The density of CoBBP was measured by a Micromeritics AccuPyc 1330 electronic density balance..

2.6. Characterization of MMMs.

Scanning electron microscopy (SEM). The morphologies of the cross and surface section of the membranes were inspected by SEM using a JEOL Model JSM-6700F scanning electron microscope (JEOL, Japan). The samples were fixed on the sample holder and sputtered with gold prior to test and then viewed with the microscopy at 10 kV.

X-ray diffraction (XRD) was analyzed using a PANAlytical X'pert pro (PAN alytical, The Netherlands) the scanning range of 2θ between5° and 40° using Cu Kα as the source of radiation.

Attenuated Total Reflectance-Fourier Transforms Infrared Spectroscopy (ATR-FTIR): The chemical structure of the membrane was inspected by FTIR. FTIR spectrum

analysis was carried out using MAGNA-560 manufactured by Thermo Nicolette Corporation (U.S.A.). ATR-FTIR spectrum was obtained in the range of wavenumbers from 4000 to 400 cm^{-1} with a scan per sample. All the samples to be measured were cut into the appropriate size and fixed on the sample table after the drying treatment, the repetition times of scan were 10.

Mechanical properties of membranes were obtained through tensile test on Instron Mechanical Tester (Testometric 350 AX) with the size of 2.0cm×4.0cm at an elongation rate of 10 mm min^{-1} under ambient temperature.

2.7. Gas permeation experiments.

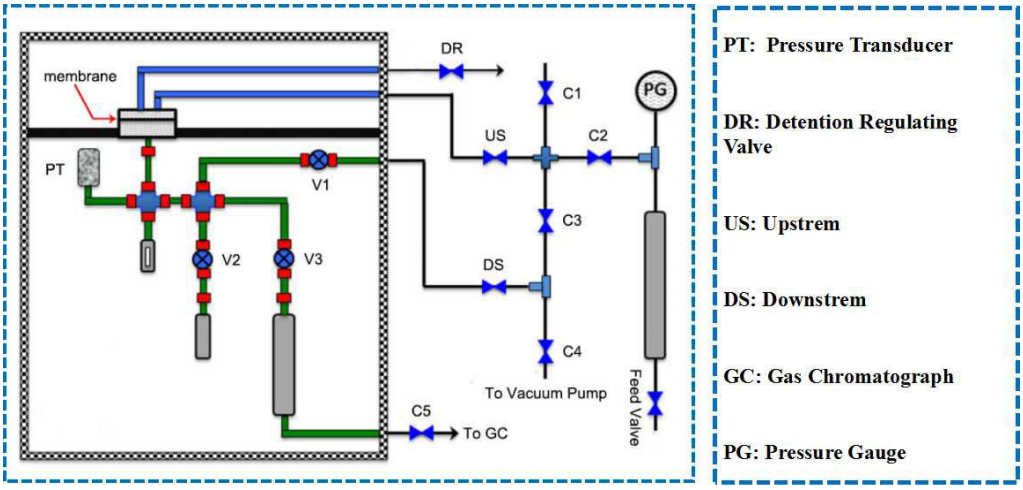

Fig. 3. Schematic diagram of mixed matrix membrane gas permeability test apparatus.

In this work, the single gas permeation testing was conducted by a gas permeation rig (FHM-PermCell-Lab) (Fig. 3). The gas transport properties were measured via variable-pressure constant-volume method.[40, 41] The prepared membrane was fixed on the flat frame, and sealed with vacuum fat and double rubber O-rings., The pure gas (CO_2 and N_2) were tested with different feed pressure (ranged from 1bar to 5bar) at constant temperature of 35°C. The gas permeability (P) was calculated from the following equation:

$$P = \frac{273\times10^{10}}{760} \times \frac{V\cdot L}{AT(\frac{P_0\cdot 76}{14.7})} \times \frac{dp}{dt} \qquad (1)$$

Where P is the gas permeability (1 Barrer $= 1 \times 10^{-10}$cm^3(STP)cm/(cm$^2 \cdot$ s $\cdot$ Hg), V is the volume of the downstream chamber (25.33 cm^3), A refers to the effective area of the membrane (cm^2), L is the effective thickness (cm), T is the operating temperature (K), P_0 is the operating pressure of the upstream chamber (psi) and dp/dt is the pressure increase rate measured by the pressure sensor in the low-pressure downstream chamber (mmHg/s).

the ideal selectivity of CO_2 over N_2 (CO_2/N_2) is calculated by :

$$\alpha_{CO2/N2} = \frac{P_{CO_2}}{P_{N_2}} \qquad (4)$$

2.8. Modelling

The CO_2 and N_2 permeability in Pebax-CoBBP were back-calculated via the Maxwell model, which is the most widely used model to predict the permeability of the composite materials:

$$P_{MMM} = P_p[\frac{P_s+2P_p-2\Phi_s(P_p-P_s)}{P_S+2P_p+\Phi_s(P_p-P_s)}] \qquad (5)$$

Where P_{MMM} is the permeability in the mixed matrix membrane; P_P is the permeability of the pure Pebax membrane; P_S is the permeability in the molecule sieve; and Φ_s is the volume fraction of molecule sieve in the polymer membrane.[42, 43]

The volume fraction Φ_s of CoBBP in the MMMs is defined as:

$$\Phi_s = \frac{m_s/\rho_s}{m_s/\rho_s + m_c/\rho_c} \qquad (6)$$

Where m_s and ρ_s refer to the mass and denisty of the contious phase (Pebax) and dispered phase (CoBBP), respectively. In most cases, the void volume can be neglected.[44] Consequently, the apparent volume fraction is approximately equal to the true volume fraction of the CoBBP in the MMMs.

3. Results and discussion.

3.1. Characterization of CoBBP.

The FTIR analysis of BBP and CoBBP were performed and shown in Fig. 5a. The spectrum of BBP shows the peak at 1593 cm^{-1} and 1610 cm^{-1} associated to the C=N and N=N vibration respectively, which are both shifted at a lower frequency (1599 and 1620 cm^{-1}) because of the formation of the mental complex. After the coordination of water molecule, a remarkable peak for the –OH vibration appears at near 3423cm^{-1} in the CoBBP complex, further confirming the formation of the complex CoBBP.

Fig. 5. (a) FTIR patterns of BBP and CoBBP; (b) TGA curve of CoBBP (insert figure: CA).

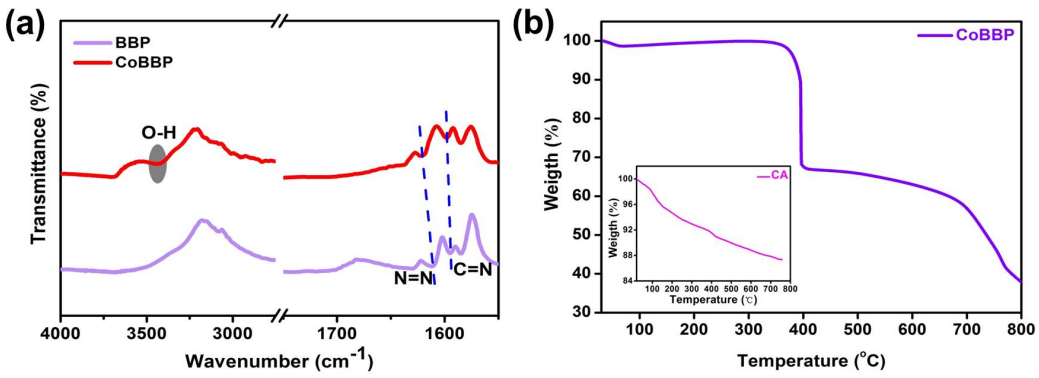

The thermal gravimetric analysis (TGA) curve of CoBBP recorded in N_2 is shown in Fig. 5b, a major mass loss is emerged at around 380°C because of the decomposition of the structure of CoBBP. The increasing temperature causes other organic group decomposed. In contrast, as the temperature rise, the mass loss of CA is occurred

gradually, and displays its instability (insert figure). Therefore, the biomimetic material CoBBP keep good thermal stability, which is superior to CA.

3.2. Characterization of MMMs.

The morphology of as-prepared membranes was characterized via SEM. The pristine Pebax membrane shows the relative smooth without any agglomerations (Fig. 6a), and the Pebax-CoBBP MMMs displays the similar morphology relative to the pristine membrane (Fig. 6e), which can be attributed to the below two reasons. First, the CoBBP nanoparticles are completely dispersed into the Pebax phase, both of them had excellent compatibility. Then, the additions of CoBBP are rarely small compared to neat Pebax. Moreover, the EDS mappings of Pebax (Fig. 6b, 6c and 6d) and Pebax-CoBBP MMMs (Fig. 6f, 6g, 6h and 6i) prove that CoBBP has been added into the Pebax phase successfully, and has distributed uniformly. (Fig. 6i) The TEM image of CoBBP nanoparticles is shown in Fig. 6j, which are emerged to the amorphous structure.

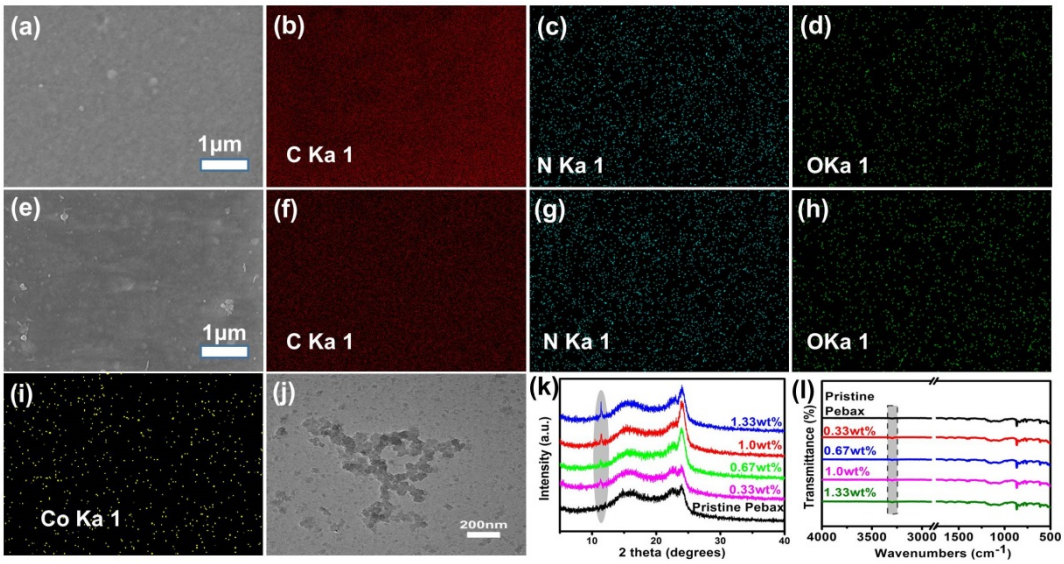

Fig. 6. Images of (a) pristine Pebax membrane; (e) Pebax-CoBBP(20) membrane; SEM and EDS mapping images of pristine Pebax membrane (b-d) and Pebax-CoBBP(20) membrane (f-i); (j) TEM image of CoBBP nanoparticles; (k) XRD patterns of pristine Pebax and other mixed matrix

membranes contained CoBBP of different loadings; (l) FTIR spectrums of pristine Pebax membrane and the MMMs with different CoBBP loadings.

The XRD patterns of the MMMs could reflect the crystal structure of polymer and the nanofillers. The broad peaks represent the material of amorphous, and the narrow peaks indicate the crystalline nature of the materials. As shown in Fig. 6k, the broader peak that ranges from 14.2° to 17.1° illustrates the soft phase of PEO, and the distinct peak at 24.0° indicates the crystalline PA phases. However, the patterns of mixed matrix membranes with different CoBBP loadings are relatively unchanged, it demonstrates that the crystalline structure is preserved.[41] After introducing the CoBBP into the Pebax matrix, the CoBBP shows its characteristic band at near $2\theta=11°$ in the MMMs. Furthermore, the increasing loadings of CoBBP in the membrane lead to an increase in peak intensity.

The FTIR analysis of neat Pebax and different mass gradients Pebax-CoBBP MMMs are shown in Fig. 6l. As we can see, there are no appearance of new peaks because of the physical blend between the continuous phase (Pebax) and dispersed phase (CoBBP). However, after incorporating the CoBBP into Pebax, the peaks at 3299cm^{-1} are enhanced gradually due to the addition of the CoBBP, because the contents of the O-H increased with the addition of the CoBBP and it demonstrates that the formation of Hydrogen bond between CoBBP and Pebax substrate at the same time. Moreover, the macroscopic phenomena shows the increased mechanical properties, which would be further proved in the test of mechanical stability of the membranes.

3.4. The mechanical stability of the membranes.

In order to test the mechanical stability of the membranes with different additives of

CoBBP, the pristine Pebax, Pebax-CA and Pebax-CoBBP were measured with the Yong's modulus, respectively.(Fig. 7a) As we can see, because the rigidity PA segment provides the mechanical properties, all of them show good flexibility. After introducing the CoBBP nanoparticles into the membranes, both the elongation and strength of the membranes increase, this is attributed to the fact that CoBBP and PA segment formed the hydrogen bonds. (Fig. 7b)

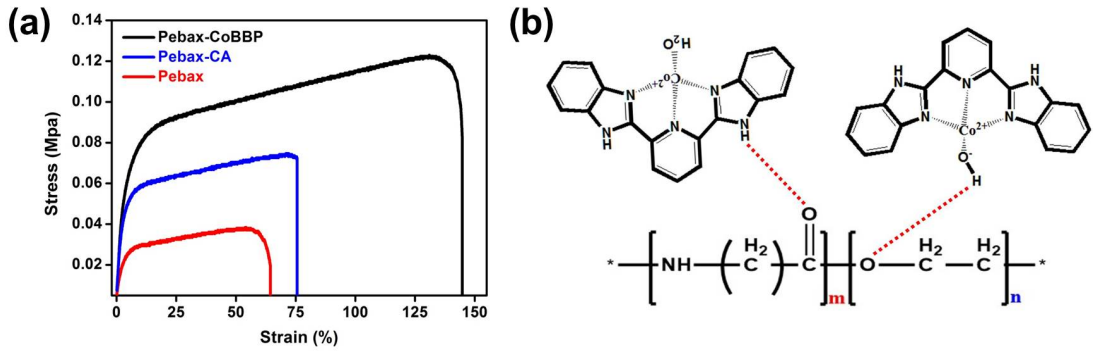

Fig. 7. (a) The stress–strain curves of the pristine Pebax membrane, Pebax-CA membrane and Pebax-CoBBP membrane; (b) the formation of hydrogen bonds between CoBBP and PA segment.

3.5. Gas separation of the MMMs.

To test whether the CoBBP can promote the transmission of CO_2 in the membranes, a control experiment of Pebax-CoBBP and pure Pebax was conducted with the same conditions, and the results are shown in Fig. 8. As we can see, when the feed pressure is 5 bar, compared with the neat Pebax membrane, the CO_2 permeability and CO_2/N_2 selectivity of the CoBBP modified membrane increase 4.2 folds (from 155.6 to 675.5barrer) and 1.2 folds (ranged from 51 to 62), respectively. This is attributed to the affinity of CoBBP to CO_2, the CoBBP fixed in the membrane can accelerate the hydration of CO_2 with the help of the free water in the membrane, and it causes to the

improved CO_2 permeability. As the result, the selectivity of CO_2/N_2 increases because the affinity of CoBBP for CO_2 is superior to N_2.

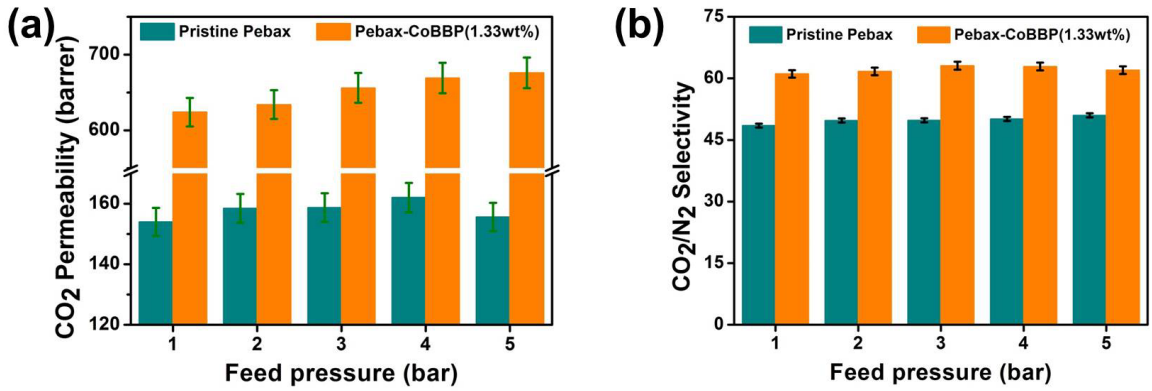

Fig. 8. CO_2 permeability and the CO_2/N_2 selectivity of pristine Pebax membranes and Pebax-CoBBP(1.33wt%) mixed matrix membrane.

3.6. The effect of CoBBP loadings.

In order to investigate the effect of CoBBP addition in the MMMs, the membranes with different loadings (0.33wt%, 0.67wt%, 1.0wt% and 1.33wt%) were prepared. As shown in Fig. 9a, the permeability of CO_2 increase with the higher amounts of CoBBP, it suggests that the more CoBBP can speed up the transmission of CO_2 in the membrane. At the same time, the CoBBP nanoparticles lead to the swelling of the MMMs. Consequently, the N_2 permeability increases slightly, but its increasing rate is far slower than CO_2. (Fig. 9b) Lastly, the final CO_2/N_2 selectivity improves. (Fig. 9c) In general, the MMMs prepared in this work display an optimum CO_2 permeability of 675.5barrer and the CO_2/N_2 selectivity of 62, surpassing the Robeson upper bond in 2008. (Fig. 9d) Compared with the pristine Pebax membrane and other MMMs based on Pebax substrate in literature, the as-prepared membranes with CoBBP nanoparticles all show high CO_2 permeability and fine CO_2/N_2 selectivity. (Table 1)

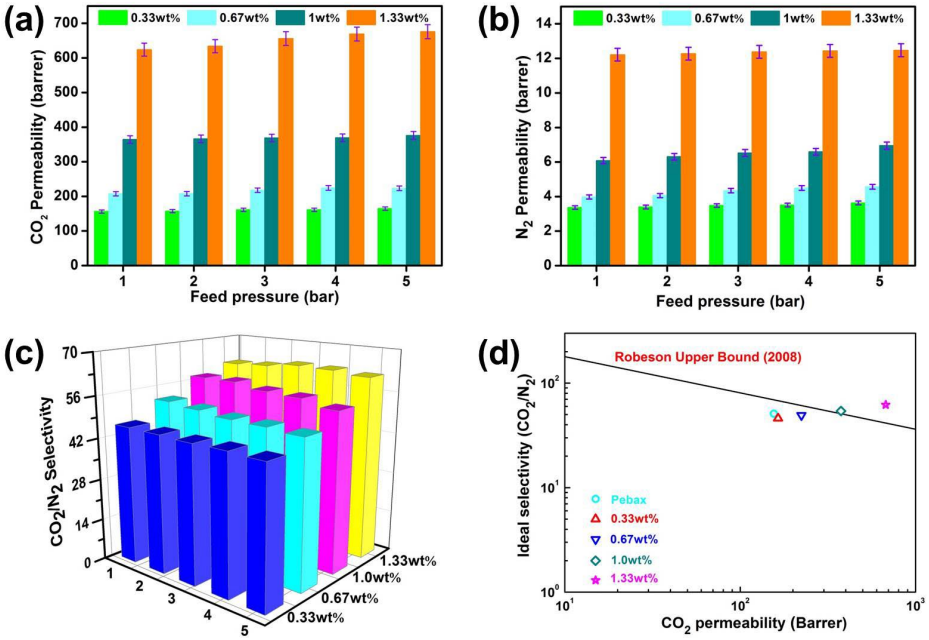

Fig. 9. CO_2 (a); N_2 (b) permeability and CO_2/N_2 selectivity (c) of the membranes with different CoBBP loadings (0.33wt%, 0.67wt%, 1.0wt% and 1.33wt%); and (d) the relationship between the CO_2 permeability and the CO_2/N_2 selectivity of the MMMs prepared in this work.

Table1 Comparison of the separation performance of other MMMs based on Pebax substrate in literature with our current work under dry state.

Membrane materials	Testing conditions	P(CO_2) barrer	CO_2/N_2 selectivity	Ref.
Pebax-PEG-PEI-GO	0.2MPa,30°C	145	62	[45]
Pebax-GO	0.3MPa,25°C	100	91	[46]
Pebax-PRG	0.2MPa,30°C	119	104	[47]
Pebax-imGO	0.8MPa,25°C	76.2	105.5	[9]
Pebax-PEG50	30°C	151	47	[48]
Pebax-MWNT	0.23MPa,21°C	105	72.4	[49]
Pebax-PDMS-MoS_2	0.2MPa,30°C	64	93	[50]
Pebax-[emim][BF_4]	0.3MPa,35°C	146.1	63	[51]
Pebax/Ag/[Bmim][BF_4]	1MPa,35°C	180	61	[52]
Pebax-NIPAM-CNTs	2atm,25°C	567	70	[53]
Pebax-MCM41-15	0.2MPa,25°C	108	53	[54]
Pebax-CoBBP	0.5MPa,30°C	675	62	This work

Furthermore, we used Maxwell model to predicate the gas permeation properties of the MMMs prepared with high loadings (1.0wt% and 1.33wt%) in this work. Fig. 10 shows the CO_2 permeability and CO_2/N_2 ideal selectivity of the MMMs predicated via Maxwell model. The back-calculated causes to the CO_2 permeability of 483barrer (1.0wt% loading) and 768barrer (1.33wt% loading) respectively, both agree with the experimental permeation results. So we can use this model to predicate the gas performance of the mixed matrix membranes with higher CoBBP loadings.

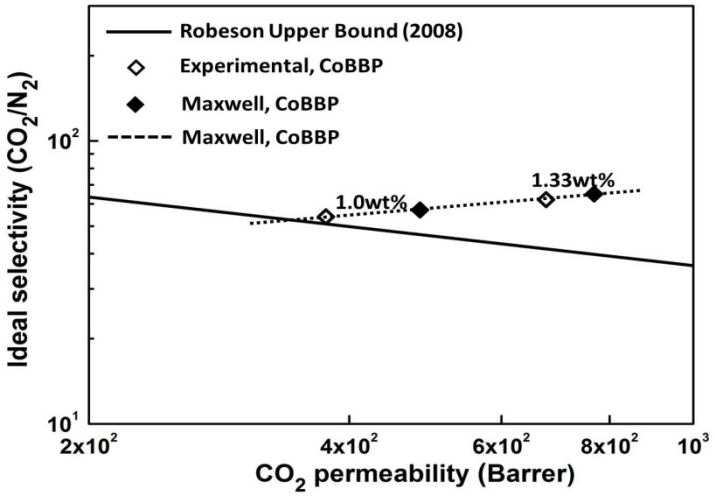

Fig. 10. Experimental and Maxwell model predicted permeation properties of Pebax-CoBBP mixed matrix membranes.

3.7. The mechanism of CoBBP.

CA can primarily catalyze the hydration of CO_2 reversibly, and it is a kind of enzyme, which contains metal ion (Zn^{2+}), with the fastest catalyze rate at present. In this work, we synthesized a biomimetic enzyme (CoBBP) with the similar structure to CA. Though the metal active site of CoBBP is differed from CA, the CoBBP also shows the affinity to CO_2. The mechanism of CoBBP catalyzes the hydration of CO_2 is similar to CA. In briefly, the OH^- connected with Co^{2+} could coordinate with CO_2 molecules, which is caused by the deprotonation of bonded water. During the hydration of CO_2, the, the His_3CoOH acts as the active substance, while in the dehydration process of catalyze, the His_3CoOH_2 is the active substance. (Fig. 11)

The related reaction equations are as follows:

$$E \cdot CoOH^- + CO_2 \leftrightarrow CoHCO_3^- \quad (7)$$

$$E \cdot CoH_2O \leftrightarrow ECoOH + H^+ \quad (8)$$

$$E \cdot CoHCO_3^- + H_2O \leftrightarrow ECoH_2O + HCO_3^- \quad (9)$$

In summary,

$$CO_2 + H_2O \leftrightarrow H^+ + HCO_3^- \qquad (10)$$

In addition, the secondary amine of CoBBP can act as the carrier to promote the facilitated traonsport of CO_2 through the mixed matrix membrane. The mechanism is described as follows:

$$CO_2 + 2R_2NH \leftrightarrow R_2NCOO^- + R_2NH_2^+ \qquad (11)$$

Fig. 11. The mechanism of CoBBP affined to CO_2.

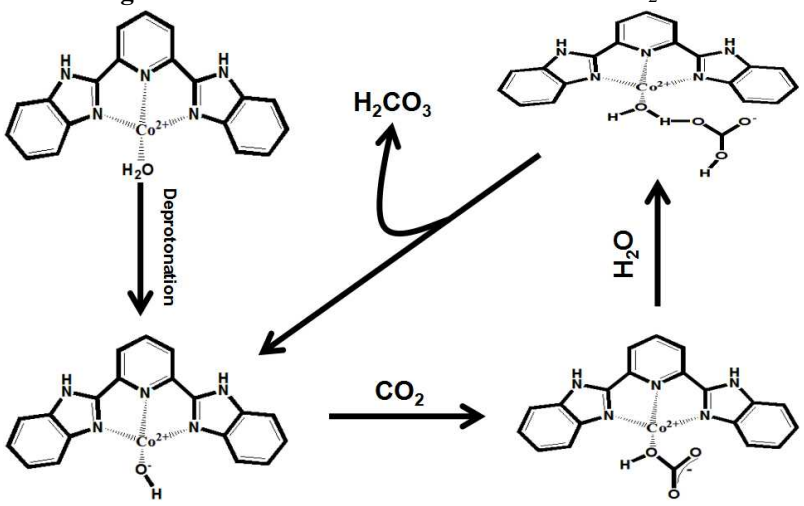

3.8 The thermal and long-term stability of MMMs with CoBBP.

Different MMMs incorporated with CoBBP and CA were incubation at a range of temperatures, (80ºC, 100ºC and 120ºC). As we can see in Fig. 12a, after a series of high temperature treatments, the membrane with CoBBP maintains the high CO_2 permeability, while the membrane with CA presents a significant decrease of CO2 permeability, In a further set of experiments at 120ºC, the CA lost activity completely, and the permeability is similar to that of the pristine Pebax membrane. This result indicates that CoBBP has higher thermal stability compared to CA to retain its affinity to CO_2 at high temperature operating conditions. Therefore, CoBBP can be a promising alternative to CA for making efficient membranes in CO_2 capture.

Furthermore, the long-term stability of the membranes with optimum performance is tested, and the result is shown in Fig. 12b. It can be seen that the membrane keeps stable CO_2 permeability and CO_2/N_2 selectivity, which indicates the outstanding structural stability and anti-aging behavior.

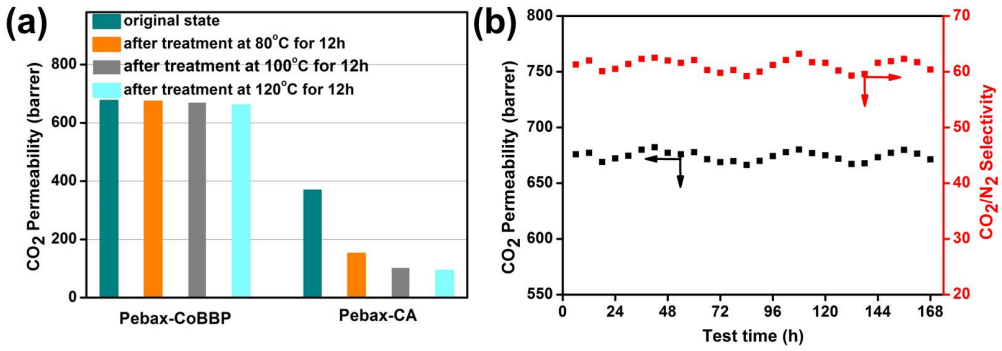

Fig. 12. (a) The comparison of CoBBP and CA after treatment at high temperature (80°C, 100°C and 120°C); (b) the stability test of the Pebax-CoBBP (1.33wt%) for up to one week and the feed pressure was 5 bar.

Conclusion

In summary, an alternative biomimetic enzyme of CoBBPwas successfully synthesized via mimicing the active site of CA. The CoBBP has a similar structure to CA, but a different mental active site . Compared to CA, the CoBBP shows excellent thermal stability after high temperature treatment. , and well remedying the defects of inactivation and expensive to CA. different MMMs with various CoBBP nanoparticles loadings were fabricated and tested. Compared to the pure Pebax membrane, the designed MMMs showed both high CO_2 permeability and high CO_2/N_2 selectivity. The highest CO_2 permeability of 675.9 Barrer and CO_2/N_2 selectivity of 62 was achieved at the optimal CoBBP loading of 1.33% . The obtained membranes characterization results demonstrate the formation of hydration bond between CoBBP and PA chains,

improving the rigidity of the MMMs, which guarantees the operational mechanical stability in the real application. In addition, the long-term stability of the membranes shows stable gas permeability, indicating excellent anti-aging property. The developed CoBBP provides a novel alternative to CA, and can potentially expand new strategy for the fabrication of biomimetic membranes for promising CO_2 capture.

Acknowledgments

This work was financially sponsored by the National Natural Science Foundation of China (No. 21376225 and 21476215), Program for Science & Technology Innovation Talents in Universities of Henan Province (16HASTIT004) and Excellent Youth Development Foundation of Zhengzhou University (No.1421324066).

References

[1] A. Brunetti, F. Scura, G. Barbieri, E. Drioli, Membrane technologies for CO2 separation, Journal of Membrane Science, 359 (2010) 115-125.

[2] S. Wang, X. Wang, Imidazolium Ionic Liquids, Imidazolylidene Heterocyclic Carbenes, and Zeolitic Imidazolate Frameworks for CO2 Capture and Photochemical Reduction, Angewandte Chemie, 55 (2016) 2308.

[3] D.M. D'Alessandro, B. Smit, J.R. Long, Carbon dioxide capture: prospects for new materials, Angew Chem Int Ed Engl, 49 (2010) 6058-6082.

[4] Z. Kang, M. Xue, L. Fan, L. Huang, L. Guo, G. Wei, B. Chen, S. Qiu, Highly selective sieving of small gas molecules by using an ultra-microporous metal–organic framework membrane, Energy Environ. Sci., 7 (2014) 4053-4060.

[5] L.M. Robeson, The upper bound revisited, Journal of Membrane Science, 320 (2008) 390-400.

[6] J. Sánchez-Laínez, B. Zornoza, S. Friebe, J. Caro, S. Cao, A. Sabetghadam, B. Seoane, J. Gascon, F. Kapteijn, C. Le Guillouzer, G. Clet, M. Daturi, C. Téllez, J. Coronas, Influence of ZIF-8 particle size in the performance of polybenzimidazole mixed matrix membranes for pre-combustion CO 2 capture and its validation through interlaboratory test, Journal of Membrane Science, 515 (2016) 45-53.

[7] V. Nafisi, M.-B. Hägg, Development of dual layer of ZIF-8/PEBAX-2533 mixed matrix membrane for CO2 capture, Journal of Membrane Science, 459 (2014) 244-255.

[8] X. Wu, Z. Tian, S. Wang, D. Peng, L. Yang, Y. Wu, Q. Xin, H. Wu, Z. Jiang, Mixed matrix membranes comprising polymers of intrinsic microporosity and covalent organic framework for gas separation, Journal of Membrane Science, 528 (2017) 273-283.

[9] Y. Dai, X. Ruan, Z. Yan, K. Yang, M. Yu, H. Li, W. Zhao, G. He, Imidazole functionalized graphene oxide/PEBAX mixed matrix membranes for efficient CO2 capture, Separation and Purification Technology, 166 (2016) 171-180.

[10] Z. Tian, S. Wang, Y. Wang, X. Ma, K. Cao, D. Peng, X. Wu, H. Wu, Z. Jiang, Enhanced gas separation performance of mixed matrix membranes from graphitic carbon nitride nanosheets and polymers of intrinsic microporosity, Journal of Membrane Science, 514 (2016) 15-24.

[11] J. Dechnik, J. Gascon, C. Doonan, C. Janiak, C.J. Sumby, New directions for mixed‐matrix membranes, Angewandte Chemie, (2017).

[12] B. Seoane, J. Coronas, I. Gascon, M.E. Benavides, O. Karvan, J. Caro, F. Kapteijn, J. Gascon, Metal-organic framework based mixed matrix membranes: a solution for highly efficient CO2 capture?, Chemical Society Reviews, 44 (2015) 2421.

[13] G. Dong, Y. Zhang, J. Hou, J. Shen, V. Chen, Graphene oxide nanosheets based novel facilitated transport membranes for efficient CO2 capture, Industrial & Engineering Chemistry Research, 55 (2016) 5403-5414.

[14] H.C. Yang, J. Hou, V. Chen, Z.K. Xu, Surface and interface engineering for organic–inorganic composite membranes, Journal of Materials Chemistry A, 4 (2016).

[15] M. Sarfraz, M. Ba-Shammakh, Synergistic effect of adding graphene oxide and ZIF-301 to polysulfone to develop high performance mixed matrix membranes for selective carbon dioxide separation from post combustion flue gas, Journal of Membrane Science, 514 (2016) 35-43.

[16] C. Ji, J. Hou, V. Chen, Cross-linked carbon nanotubes-based biocatalytic membranes for micro-pollutants degradation: Performance, stability, and regeneration, Journal of Membrane Science, 520 (2016) 869-880.

[17] J. Hou, G. Dong, B. Xiao, C. Malassigne, V. Chen, Preparation of titania based biocatalytic nanoparticles and membranes for CO2conversion, J. Mater. Chem. A, 3 (2015) 3332-3342.
[18] J. Hou, M.Y. Zulkifli, M. Mohammad, Y. Zhang, A. Razmjou, V. Chen, Biocatalytic gas-liquid membrane contactors for CO 2 hydration with immobilized carbonic anhydrase, Journal of Membrane Science, 520 (2016) 303-313.
[19] B.K. Shanbhag, B. Liu, J. Fu, V.S. Haritos, L. He, Self-Assembled Enzyme Nanoparticles for Carbon Dioxide Capture, Nano Letters, 16 (2016) 3379.
[20] F.B. Rehm, S. Chen, B.H. Rehm, Enzyme Engineering for In Situ Immobilization, Molecules, 21 (2016) 1370.
[21] Y. Zhang, H. Wang, J. Liu, J. Hou, Y. Zhang, Enzyme-embedded metal–organic framework membranes on polymeric substrates for efficient CO2 capture, J. Mater. Chem. A, 5 (2017) 19954-19962.
[22] K. Min, J. Kim, K. Park, Y.J. Yoo, Enzyme immobilization on carbon nanomaterials: Loading density investigation and zeta potential analysis, Journal of Molecular Catalysis B: Enzymatic, 83 (2012) 87-93.
[23] D. Sivanesan, M.H. Youn, A. Murnandari, J.M. Kang, K.T. Park, H.J. Kim, S.K. Jeong, Enhanced CO 2 absorption and desorption in a tertiary amine medium with a carbonic anhydrase mimic, Journal of Industrial and Engineering Chemistry, 52 (2017) 287-294.
[24] P.C. Sahoo, Y.N. Jang, S.W. Lee, Enhanced biomimetic CO2 sequestration and CaCO3 crystallization using complex encapsulated metal organic framework, Journal of Crystal Growth, 373 (2013) 96-101.
[25] K. Yao, Z. Wang, J. Wang, S. Wang, Biomimetic material--poly(N-vinylimidazole)-zinc complex for CO2 separation, Chem Commun (Camb), 48 (2012) 1766-1768.
[26] M. Saeed, L. Deng, Carbon nanotube enhanced PVA-mimic enzyme membrane for post-combustion CO 2 capture, International Journal of Greenhouse Gas Control, 53 (2016) 254-262.
[27] G. Parkin, Synthetic analogues relevant to the structure and function of zinc enzymes, Cheminform, 35 (2004) 699.
[28] J.F. Domsic, R. Mckenna, Sequestration of carbon dioxide by the hydrophobic pocket of the carbonic anhydrases, Biochimica Et Biophysica Acta Proteins & Proteomics, 1804 (2010) 326-331.
[29] I. Nath, J. Chakraborty, F. Verpoort, Metal organic frameworks mimicking natural enzymes: a structural and functional analogy, Chem Soc Rev, 45 (2016) 4127-4170.
[30] D. Lee, Y. Kanai, Biomimetic Carbon Nanotube for Catalytic CO2 Hydrolysis: First-Principles Investigation on the Role of Oxidation State and Metal Substitution in Porphyrin, Journal of Physical Chemistry Letters, 7 (2012) 1369-1373.
[31] L.Y. Cheng, Y.T. Long, H.B. Kraatz, H. Tian, Evaluation of an immobilized artificial carbonic anhydrase model for CO2 sequestration, Chemical Science, 2 (2011) 1515-1518.
[32] P.C. Sahoo, Y.N. Jang, S.W. Lee, Immobilization of carbonic anhydrase and an artificial Zn(II) complex on a magnetic support for biomimetic carbon dioxide sequestration, Journal of Molecular Catalysis B Enzymatic, 82 (2012) 37-45.
[33] E. Kimura, T. Shiota, T. Koike, M. Shiro, M. Kodama, A Zinc(II) Complex of 1,5,9-triazacyclododecane ([12]aneN3) as a model for carbonic anhydrase, Cheminform, 21 (1990) 5805-5811.
[34] X. Zhang, R.V. Eldik, T. Koike, E. Kimura, Kinetics and mechanism of the hydration of carbon dioxide and dehydration of bicarbonate catalyzed by a zinc (II) complex of 1,5,9-triazacyclododecane as a model for carbonic anhydrase, Inorganic Chemistry, 32 (1993) 5749-5755.
[35] X. Zhang, R.V. Eldik, A functional model for carbonic anhydrase: thermodynamic and kinetic study of a tetraazacyclododecane complex of zinc(II), Inorganic Chemistry, 34 (1995) 5606-5614.
[36] Y. Wang, H. Li, G. Dong, C. Scholes, V. Chen, Effect of Fabrication and Operation Conditions on CO2

Separation Performance of PEO–PA Block Copolymer Membranes, Industrial & Engineering Chemistry Research, 54 (2015) 7273-7283.
[37] L. Wang, Y. Li, S. Li, P. Ji, C. Jiang, Preparation of composite poly(ether block amide) membrane for CO2 capture, Journal of Energy Chemistry, 23 (2014) 717-725.
[38] J. Cheng, L. Hu, C. Ji, H. Zhou, K. Cen, Porous Ceramic Hollow Fiber-Supported Pebax/PEGDME Composite Membrane for CO2 Separation from Biohythane, Rsc Advances, 5 (2015) 60453-60459.
[39] B. Chen, C. Liang, J. Yang, D.S. Contreras, Y.L. Clancy, E.B. Lobkovsky, O.M. Yaghi, S. Dai, A Microporous Metal–Organic Framework for Gas‐Chromatographic Separation of Alkanes, Angewandte Chemie, 118 (2006) 1390-1393.
[40] P. Tin, Effects of cross-linking modification on gas separation performance of Matrimid membranes, Journal of Membrane Science, 225 (2003) 77-90.
[41] W.H. Lin, R.H. Vora, T.S. Chung, Gas transport properties of 6FDA‐durene/1,4‐phenylenediamine (pPDA) copolyimides, Journal of Polymer Science Part B Polymer Physics, 38 (2015) 2703-2713.
[42] C. Zhang, Y. Dai, J.R. Johnson, O. Karvan, W.J. Koros, High performance ZIF-8/6FDA-DAM mixed matrix membrane for propylene/propane separations, Journal of Membrane Science, 389 (2012) 34-42.
[43] J. Liu, T.-H. Bae, W. Qiu, S. Husain, S. Nair, C.W. Jones, R.R. Chance, W.J. Koros, Butane isomer transport properties of 6FDA–DAM and MFI–6FDA–DAM mixed matrix membranes, Journal of Membrane Science, 343 (2009) 157-163.
[44] Q. Song, S.K. Nataraj, M.V. Roussenova, J.C. Tan, D.J. Hughes, W. Li, P. Bourgoin, M.A. Alam, A.K. Cheetham, S.A. Al-Muhtaseb, E. Sivaniah, Zeolitic imidazolate framework (ZIF-8) based polymer nanocomposite membranes for gas separation, Energy & Environmental Science, 5 (2012) 8359.
[45] X. Li, Y. Cheng, H. Zhang, S. Wang, Z. Jiang, R. Guo, W. Hong, Efficient CO2 Capture by Functionalized Graphene Oxide Nanosheets as Fillers To Fabricate Multi-Permselective Mixed Matrix Membranes, Acs Applied Materials & Interfaces, 7 (2015) 5528.
[46] J. Shen, G. Liu, K. Huang, W. Jin, K.R. Lee, N. Xu, Membranes with Fast and Selective Gas‐Transport Channels of Laminar Graphene Oxide for Efficient CO2 Capture, Angewandte Chemie, 54 (2015) 578.
[47] G. Dong, J. Hou, J. Wang, Y. Zhang, V. Chen, J. Liu, Enhanced CO 2 /N 2 separation by porous reduced graphene oxide/Pebax mixed matrix membranes, Journal of Membrane Science, 520 (2016) 860-868.
[48] A. Car, C. Stropnik, W. Yave, K.V. Peinemann, PEG modified poly(amide-b-ethylene oxide) membranes for CO2 separation, Journal of Membrane Science, 307 (2008) 88-95.
[49] B. Yu, H. Cong, Z. Li, J. Tang, X.S. Zhao, Pebax‐1657 nanocomposite membranes incorporated with nanoparticles/colloids/carbon nanotubes for CO2/N2 and CO2/H2 separation, Journal of Applied Polymer Science, 130 (2013) 2867-2876.
[50] Y. Shen, H. Wang, X. Zhang, Y. Zhang, MoS2 Nanosheets Functionalized Composite Mixed Matrix Membrane for Enhanced CO2 Capture via Surface Drop-Coating Method, ACS Appl Mater Interfaces, 8 (2016) 23371-23378.
[51] W. Fam, J. Mansouri, H. Li, V. Chen, Improving CO 2 separation performance of thin film composite hollow fiber with Pebax®1657/ionic liquid gel membranes, Journal of Membrane Science, 537 (2017).
[52] E.E. Ghasemi, M. Omidkhah, A.A. Ebadi, Interfacial Design of Ternary Mixed Matrix Membranes Containing Pebax 1657/Silver-Nanopowder/[BMIM][BF4] for Improved CO2 Separation Performance, Acs Applied Materials & Interfaces, 9 (2017) 10094-10105.
[53] H. Zhang, R. Guo, J. Hou, Z. Wei, X. Li, Mixed Matrix Membranes Containing Carbon Nanotubes Composite with Hydrogel for Efficient CO2 Separation, Acs Applied Materials & Interfaces, 8 (2016).
[54] H. Wu, X. Li, Y. Li, S. Wang, R. Guo, Z. Jiang, C. Wu, Q. Xin, X. Lu, Facilitated transport mixed matrix

membranes incorporated with amine functionalized MCM-41 for enhanced gas separation properties, Journal of Membrane Science, 465 (2014) 78-90.